Bending triangular finite element with a fictitious fourth node based on the strain approach

Mohammed Himeur — Mohamed Guenfoud

Civil Engineering and hydraulic Laboratory
Guelma University
24000 - Guelma, Algeria
{bet_himeur, gue2905m}@yahoo.fr

ABSTRACT. *We present a new plate bending triangular finite element. It is developed in perspective to building shell elements. Its formulation uses concepts related to the deformation approach, the fourth fictitious node, the static condensation and analytic integration. It is based on the assumptions of the theory of thin plates (Kirchhoff theory). The approach has resulted in a bending plate finite element (HIMEUR) competitive, robust and efficient.*

RESUME. *Nous présentons un élément fini nouveau de plaque triangulaire d'élasticité plane. Cet élément est développé dans la perspective de construction des éléments de coques. Sa formulation utilise des concepts relatifs à l'approche en déformation, au quatrième nœud fictif, à la condensation statique, à l'intégration analytique et se base sur les hypothèses de la théorie des plaques minces (Théorie de Kirchhoff). La démarche adoptée a permis d'aboutir à un élément fini de plaque (HIMEUR) concurrentiel, robuste et performant.*

KEYWORDS: *finite element, strain formulation, analytical integration, static condensation, thin plate.*

MOTS-CLÉS: *élément fini, formulation en déformation, intégration analytique, condensation statique, plaque mince.*

DOI:10.3166/EJCM.20.455-485

1. Introduction

Complex shell structures are frequently encountered in various fields. The development of simple and efficient finite elements for the analysis of these structures is a major thrust of scientific research in solid mechanics. Nevertheless, problems are often encountered, making difficult the achievement of the assigned objectives. The main observed constraints are often linked to the followings:

– Displacement fields incompatibility aspects when affixing the membrane elements with those of the plate.

– Both phenomena of "shear locking" and "membrane locking".

– The numerical problems induced by the absence of the "*sixth DOF*" in the case of co-planar elements.

– The numerical problems associated with numerical integration.

Many finite elements are developed for solving these problems. But most of them have remained ineffective in the analysis of arbitrary geometric configurations. Isoparametric elements are the most successful among those available due to their ability to successfully modelling curved structures. Only the phenomenon of shear locking leaves these unsuitable for the analysis of thin plates with distorted mesh. Despite the use of reduced integration and stabilization techniques of finite element in order to circumvent this problem, the developed formulations did not converge to the solutions given by the theory of thin plates and often confront the problem of singularity of the stiffness matrix.

A brief review of the literature allows us to identify, but not limited, some recent work by researchers to address these problems:

– Development of a plate element by (Barik *et al*., 2002) that has the qualities of an element in terms of isoparametric modelling capability with any mesh size, and without the disadvantage of the phenomenon of shear locking.

– The amendments made by (Chinosi, 2005) at the boundary conditions for Reissner-Mindlin plates; prevent free boundary conditions to address the problem of convergence towards the reference solution for plates of small thickness.

– The triangular shell element with six nodes based on the approach MITC developed by (Do-Nyun *et al*., 2009) is characterized by quality spatially isotopic element and the absence of zero energy modes.

The objective of this research is, "the formulation of shell finite elements based on the "deformation approach" whose purpose is to circumvent these difficulties on the one hand, and the construction of finite shell elements which are simple and effective for the analysis of complex structures, on the other hand. To do this, we have enriched our approach with the concepts and development techniques based on:

– the adoption of the "*deformation approach*";

– the introduction of a "*fictitious fourth node*",

– the elimination of the freedom degrees corresponding to the "*fictitious fourth node" by static condensation,*

– the use of "*analytic integration"* to evaluate the stiffness matrix.

Early works (Himeur, 2008) led to the construction of triangular membrane finite elements which can be easily combined with inflected elements (slabs, beams and shells). Those elements are:

– "*T3_Kteta*" (Himeur, 2008), in which the unknown nodal rotation is obtained by adding to the "CST" stiffness matrix (as expressed in stain approach), a stiffness matrix associated with rotation around the normal (drilling rotation). Starting from the (Providas *et al*., 2000) approach, this rotation matrix is obtained by minimizing the rotation strain energy around the normal.

– "*T43*" (Himeur *et al*., 2008) and "*T43_Eq*" (Himeur, 2008) are triangular finite elements with central disrupted node. They are characterized by the presence of unknown rotation nodal defined by the derivation of displacement fields (drilling rotation). The interpolation functions are those used by Sabir (Sabir, 1985) for the "*T43*" element and those obtained from the equilibrium conditions for the "*T43_Eq*" element (bi-harmonic polynomials selected from the solutions given by the (Teodorecu, 1982) Airy function development).

– "*T42*" and "*T42_Eq*" (Himeur, 2008) which do not have an unknown nodal rotations,

This on going work is a continuation for our research whose main focus this time is on the development of plate finite triangular elements. The triangular finite element inflected with a fictitious fourth node based on the deformation approach is the culmination of this above mentioned work. We call it «*HIMEUR*».

This element is formulated by using the deformation approach. The interpolation functions of the deformation fields (consequently, displacements and stresses) are developed by using Pascal's triangle. It is a triangular element to which we added a fourth fictitious node positioned outside and away from the triangle. This position, outside, is thus chosen to avoid the relaxation of the stiffness matrix resulting in an overestimation of the nodal displacements. The freedom degrees corresponding to the fourth node are then eliminated by the static condensation of the stiffness matrix at the elementary level. So the main interest of this fictitious node lies on the enrichment of the displacement field (p refinement *i.e.*: increase in the degree of the polynomial interpolation), which consequently aims at a greater precision in the approximation of the solution. The corresponding variational criterion is that of the total potential energy. The analytical integration for the evaluation of the stiffness matrix is highly interesting to avoid the loss of convergence phenomenon observed in isoparametric elements which use numerical integration and are very sensitive (their convergence is conditioned by a regular mesh - undistorted). The assumption of this formulation is that of the thin plate theory (Kirchhoff's theory). This latter neglects the effect of transverse shear.

In a bid to validate the new HIMEUR element, we have undertaken a set of test cases. For each test case, the result is compared, on one hand, to the corresponding reference solution, and on the other hand, the solution is given by certain plate elements found in existing literature. The behaviour in pure bending (bending to the dominant shear) is treated through the example used by J.-L. Batoz and Dhatt G. (Batoz *et al.*, 1990). This test proves very useful to evaluate the convergence levels, robustness and performance of our element. The behaviour of this element, relative to the transverse shear, is analyzed by using the example treated by Guenfoud (Guenfoud, 1993), Belarbi and Sharif (Belarbi *et al.*, 1999). We have ultimately submitted our element to the tests suggested by Robinson (Robinson, 1978) to gauge its behaviour to the torsion aspects.

On the whole, the approach in our development has resulted in a competitive, robust and efficient (*HIMEUR*) plate finite element. This is visible, first, through its excellent convergence rhythm towards the reference solution, and secondly, through its behaviour performances towards other triangular plate elements in the existing literature: DKT, HCT (Batoz *et al.*, 1990), C^O (Belytschko, 1984), ANST3 (Guenfoud, 1990), ANST6 (Guenfoud, 1990), TRUMP (Argyris *et al.*, 1977) and SRI (Sabourin *et al.*, 2000).

2. Basic equations of the thin plates theory (Kirchhoff theory)

2.1. *Kinematics equations*

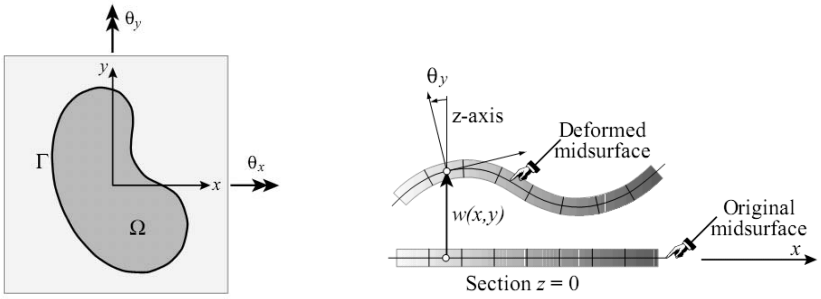

Figure 1. *Deformation of a bending plate (Kirchhoff Theory)*

In Figure 1, the rotations around the two axes x and y are denoted θ_x and θ_y , and slopes in both directions are defined by the variables β_x and β_y, with:

$$\beta_x = \theta_y \qquad \beta_y = -\theta_x \qquad [1]$$

The assumption of the cross section implies a linear variation of the displacement over the thickness of the plate. What is translated by:

$$u(x,y,z) = z\beta_x(x,y) = z\theta_y(x,y),$$
$$v(x,y,z) = z\beta_y(x,y) = -z\theta_x(x,y),$$
$$w(x,y,z) = w(x,y) \qquad [2]$$

The expressions [2] permit to uncouple the displacement (u, v) and the arrow (w) is in reference to the assumptions of Kirchhoff, the only field to define the behaviour of the plate. Thus, the displacements are given by:

$$u = -z\frac{\partial w}{\partial x} \qquad v = -z\frac{\partial w}{\partial y} \qquad [3]$$

And the rotations are given by:

$$-\theta_x = \beta_y = -\frac{\partial w}{\partial y} \qquad \theta_y = \beta_x = -\frac{\partial w}{\partial x} \qquad [4]$$

The infinitesimal strain tensor is then:

$$\varepsilon_x = \frac{\partial u}{\partial x} = z\frac{\partial \beta_x}{\partial x} = -z\frac{\partial^2 w}{\partial x^2} \quad \varepsilon_y = \frac{\partial v}{\partial y} = z\frac{\partial \beta_y}{\partial y} = -z\frac{\partial^2 w}{\partial y^2}$$
$$\gamma_{xy} = \frac{\partial u}{\partial y} + \frac{\partial v}{\partial x} = z\left(\frac{\partial \beta_x}{\partial y} + \frac{\partial \beta_y}{\partial x}\right) = -2z\frac{\partial^2 w}{\partial x \partial y} \qquad [5]$$
$$\gamma_{xz} = \gamma_{yz} = 0$$

Moments related to the bending curvatures are given by:

$$K_x = \frac{\partial \beta_x}{\partial x} = -\frac{\partial^2 w}{\partial x^2} \qquad K_y = \frac{\partial \beta_y}{\partial y} = -\frac{\partial^2 w}{\partial y^2} \qquad [6]$$
$$K_{xy} = \left(\frac{\partial \beta_x}{\partial y} + \frac{\partial \beta_y}{\partial x}\right) = -2\frac{\partial^2 w}{\partial x \partial y}$$

2.2. *Kinematics compatibility conditions*

These conditions were established by St. Venant (1854) (Frey, 1998). Their satisfaction is required to guarantee the uniqueness of the displacements. The compatibility equations are as developed as follows:

$$\frac{\partial^2 K_x}{\partial y^2} + \frac{\partial^2 K_y}{\partial x^2} = \frac{\partial^2 K_{xy}}{\partial x \partial y}$$

$$\frac{\partial^2 \gamma_{xz}}{\partial x \partial y} - \frac{\partial^2 \gamma_{yz}}{\partial x^2} + \frac{\partial^2 K_{xy}}{\partial x} = 2\frac{\partial K_x}{\partial y}$$

$$\frac{\partial^2 \gamma_{yz}}{\partial x \partial y} - \frac{\partial^2 \gamma_{xz}}{\partial y^2} + \frac{\partial^2 K_{xy}}{\partial y} = 2\frac{\partial K_y}{\partial x} \qquad [7]$$

2.3. *Constitutive law*

In plane state of stress and for isotropic materials, generally accepted hypothesis for the calculation of thin structures (beams, plates and shells), the constitutive law is written:

$$\begin{Bmatrix} \sigma_x \\ \sigma_y \\ \tau_{xy} \end{Bmatrix} = \frac{E}{1-\nu^2} \begin{bmatrix} 1 & \nu & 0 \\ \nu & 1 & 0 \\ 0 & 0 & \frac{1-\nu}{2} \end{bmatrix} \begin{Bmatrix} \varepsilon_x \\ \varepsilon_y \\ \gamma_{xy} \end{Bmatrix}. \quad [8]$$

This translates in terms of relationship "*moment-curvature*" by the following equation system:

$$\begin{Bmatrix} M_x \\ M_y \\ M_{xy} \end{Bmatrix} = \frac{Eh^3}{12(1-\nu^2)} \begin{bmatrix} 1 & \nu & 0 \\ \nu & 1 & 0 \\ 0 & 0 & \frac{1-\nu}{2} \end{bmatrix} \begin{Bmatrix} K_x \\ K_y \\ K_{xy} \end{Bmatrix} = \frac{Eh^3}{12(1-\nu^2)} \begin{bmatrix} 1 & \nu & 0 \\ \nu & 1 & 0 \\ 0 & 0 & \frac{1-\nu}{2} \end{bmatrix} \begin{Bmatrix} -\frac{\partial^2 w}{\partial x^2} \\ -\frac{\partial^2 w}{\partial y^2} \\ -2\frac{\partial^2 w}{\partial x \partial y} \end{Bmatrix} \quad [9]$$

2.4. *Equations of equilibrium*

The balance of an element of dimensions $dx \times dy$ is obtained by the balance of forces of internal and external actions.

$$q dx dy + (Q_x + \frac{\partial Q_x}{\partial x}) dy + (Q_y + \frac{\partial Q_y}{\partial y}) dx - Q_x dy - Q_y dx = 0 \quad [10]$$

where Q_x and Q_y are the shear forces in the sections perpendicular to the axes x and y respectively; the expression [10] is simplified to give:

$$q + \frac{\partial Q_x}{\partial x} + \frac{\partial Q_y}{\partial y} = 0 \quad [11]$$

The balance of moments about the axes x and y gives:

$$Q_x = \frac{\partial M_x}{\partial x} + \frac{\partial M_{xy}}{\partial y} \qquad Q_y = \frac{\partial M_y}{\partial y} + \frac{\partial M_{xy}}{\partial x} \quad [12]$$

By replacing the Q_x and Q_y values of Equations [12] in [11] and using bending behaviour law [9], the equilibrium condition would result in the displacement function "w" by the following expression:

$$\frac{\partial^4 w}{\partial x^4} + 2\frac{\partial^4 w}{\partial x^2 \partial y^2} + \frac{\partial^4 w}{\partial y^4} - \frac{q}{D} = 0 \qquad [13]$$

with $$D = \frac{Eh^3}{12(1-\upsilon^2)}$$

3. Formulation of the element *"HIMEUR"*

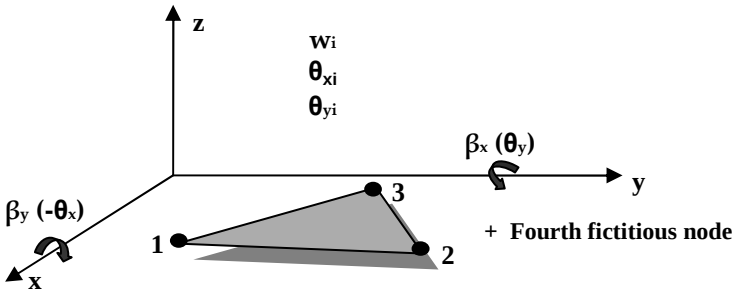

Figure 2. *Triangular plate element with w, β_x, β_y freedom degrees at each node*

3.1. *Shape function*

For rigid body motions, bending curvatures are related to zero:

$$K_x = 0 \qquad K_y = 0 \qquad K_{xy} = 0 \qquad [14]$$

By replacing in Equations [6] the curves with their values given by Equations [14] and after integration, we obtain the displacement fields representing the rigid body motions which are as follows:

$$W = a_1 - a_2.x - a_3 y \qquad \beta_x = a_2 \qquad \beta_y = a_3 \qquad [15]$$

with a_2 and a_3, parameters representing rotations θ_x and θ_y of the rigid body about respective axis "*y*" and "*x*" representing the translation and a_1 (arrow) of the rigid body along the normal (axis "*z*").

Our element has four nodes (see Figure 2): three vertices to which we have added a fourth fictitious node. Each of its nodes has three degrees of freedom. So the displacement fields, formulated by the use of the model deformation, have 12 independent constants (a_1, ..., a_{12}). The first three (a_1, a_2, a_3) are used in Equations [15] to represent rigid body motions. The other nines (a_4, ..., a_{12}) are used to represent the state of pure bending. They are divided into the deformation interpolation functions to satisfy the Equations [7] of kinematics compatibility for

plane elasticity. Thus, the deformation fields for the higher modes are derived from Pascal's triangle as follows:

$$\begin{aligned} K_x &= a_4 + a_5.x + a_6.y + a_7.x.y \\ K_y &= a_8 + a_9.x + a_{10}.y + a_{11}x.y \\ K_{xy} &= a_{12} + 2.a_6.x + a_7.x^2 + 2.a_9.y + a_{11}.y^2 \end{aligned} \quad [16]$$

By replacing in Equations [6] the curves with their values given by Equations [16] and after integration, we obtain the following field trips:

$$\begin{aligned} W &= -a_4.\frac{x^2}{2} - a_5.\frac{x^3}{6} - a_6.\frac{x^2.y}{2} - a_7.\frac{x^3.y}{6} - a_8.\frac{y^2}{2} - a_9.\frac{x.y^2}{2} - a_{10}.\frac{y^3}{6} - a_{11}.\frac{x.y^3}{6} - a_{12}.\frac{x.y}{2} \\ \beta_x &= a_4.x + a_5.\frac{x^2}{2} + a_6.x.y + a_7.\frac{x^2.y}{2} + a_9.\frac{y^2}{2} + a_{11}.\frac{y^3}{6} + a_{12}.\frac{y}{2} \\ \beta_y &= a_6.\frac{x^2}{2} + a_7.\frac{x^3}{6} + a_8.y + a_9.x.y + a_{10}.\frac{y^2}{2} + a_{11}.\frac{x.y^2}{2} + a_{12}.\frac{x}{2} \end{aligned} \quad [17]$$

The final field of displacements is obtained by adding the relations [15] and [17]:

$$\begin{aligned} W &= a_1 - a_2.x - a_3.y - a_4.\frac{x^2}{2} - a_5.\frac{x^3}{6} - a_6.\frac{x^2.y}{2} - a_7.\frac{x^3.y}{6} - a_8.\frac{y^2}{2} - a_9.\frac{x.y^2}{2} - a_{10}.\frac{y^3}{6} \\ &- a_{11}.\frac{x.y^3}{6} - a_{12}.\frac{x.y}{2} \\ \beta_x &= a_2 + a_4.x + a_5.\frac{x^2}{2} + a_6.x.y + a_7.\frac{x^2.y}{2} + a_9.\frac{y^2}{2} + a_{11}.\frac{y^3}{6} + a_{12}.\frac{y}{2} \\ \beta_y &= a_3 + a_6.\frac{x^2}{2} + a_7.\frac{x^3}{6} + a_8.y + a_9.x.y + a_{10}.\frac{y^2}{2} + a_{11}.\frac{x.y^2}{2} + a_{12}.\frac{x}{2} \end{aligned} \quad [18]$$

Matrix forms the displacement field given by Equations [18] we read it as follows:

$$\begin{Bmatrix} W(x,y) \\ \beta_x(x,y) \\ \beta_y(x,y) \end{Bmatrix} = [f(x,y)]\{a_i\} \quad [19]$$

with, $\{a_i\}^T = < a_1, a_2, a_3, a_4, a_5, a_6, a_7, a_8, a_9, a_{10}, a_{11}, a_{12} >$

$$[f(x,y)] = \begin{bmatrix} 1 & -x & -y & -\frac{x^2}{2} & -\frac{x^3}{6} & -\frac{x^2.y}{2} & -\frac{x^3.y}{6} & -\frac{y^2}{2} & -\frac{x.y^2}{2} & -\frac{y^3}{6} & -\frac{x.y^3}{6} & -\frac{x.y}{2} \\ 0 & 1 & 0 & x & \frac{x^2}{2} & x.y & \frac{x^2.y}{2} & 0 & \frac{y^2}{2} & 0 & \frac{y^3}{6} & \frac{y}{2} \\ 0 & 0 & 1 & 0 & 0 & \frac{x^2}{2} & \frac{x^3}{6} & y & x.y & \frac{y^2}{2} & \frac{x.y^2}{2} & \frac{x}{2} \end{bmatrix} \quad [20]$$

Knowing the nodal coordinates (x_i, y_i) corresponding to the nodes j (j = 1... 4) and applying the relation [20], the vector of nodal displacements at the elementary level is given as follows:

$$\{q^e\}=\begin{bmatrix}[f(x_1,y_1)]\\ [f(x_2,y_2)]\\ [f(x_3,y_3)]\\ [f(x_4,y_4)]\end{bmatrix}\{a_i\} \qquad [21]$$

with, $\{q^e\}^T = < w_1, \beta_{x1}, \beta_{y_1}, w_2, \beta_{x2}, \beta_{y_2}, w_3, \beta_{x3}, \beta_{y3}, w_4, \beta_{x4}, \beta_{y_4} >$

$[A] = \begin{bmatrix}[f(x_1,y_1)]\\ [f(x_2,y_2)]\\ [f(x_3,y_3)]\\ [f(x_4,y_4)]\end{bmatrix}$ is the matrix of nodal coordinates. It has been developed in the appendix.

From Equation [21], we deduce the value of parameters "a_i" which are given by the system of equations:

$$\{a_i\}=[A]^{-1}\{q^e\} \qquad [22]$$

By replacing the parameters which have the relationship given by [22] in the Equation system [19], we obtain the following relationship:

$$\begin{Bmatrix}W(x,y)\\ \beta_x(x,y)\\ \beta_y(x,y)\end{Bmatrix}=[f(x,y)].[A]^{-1}.\{q^e\} \qquad [23]$$

which represents the matrix of interpolation functions N_i. By replacing in Equations [6], *w(x,y)* values of Equation [19], the relationship *strain - displacement* takes the following expanded:

$$\{K\}=\begin{Bmatrix}K_x\\ K_y\\ K_{xy}\end{Bmatrix}=\begin{bmatrix}0&0&0&1&x&y&x.y&0&0&0&0&0\\ 0&0&0&0&0&0&0&1&x&y&x.y&0\\ 0&0&0&0&0&2.x&x^2&0&2.y&0&y^2&1\end{bmatrix}.\{a_i\} \qquad [24]$$

Thus, the deformation matrix [Q(x,y)] is given as follows ([K]=[Q(x,y)]{a_i}):

$$[Q(x,y)]=\begin{bmatrix}0&0&0&1&x&y&x.y&0&0&0&0&0\\ 0&0&0&0&0&0&0&1&x&y&x.y&0\\ 0&0&0&0&0&2.x&x^2&0&2.y&0&y^2&1\end{bmatrix} \qquad [25]$$

3.2. *Elementary stiffness matrix*

The internal virtual work, elementary discredited is given by the expression:

$$(\delta W_{\text{int}})^e = \int_{V^e} \delta\{\varepsilon\}^T.[\sigma].dV \qquad [26]$$

Knowing that: $$\{\varepsilon\} = [N'].\{q^e\} = [Q(x,y)].[A]^{-1}\{q^e\} \qquad [27]$$

And $$\{\sigma\} = [D].\{\varepsilon\} \qquad [28]$$

and replacing in the expression [26] $\{\varepsilon\}$ and $\{\sigma\}$ by values given respectively in Equations [27] and [28] yields :

$$(\delta W_{\text{int}})^e = \delta\{q^e\}^T \int_V [Q(x,y)]^T.[A^{-1}]^T.[D].[Q(x,y)].[A]^{-1}\{q^e\}dV \qquad [29]$$

Thus, the elementary stiffness matrix derived from the expression [29] is as follows:

$$[K^e] = \int_V [Q(x,y)]^T.[A^{-1}]^T.[D].[Q(x,y)].[A]^{-1} dV \qquad [30]$$

The expression [30] can be written:

$$[K^e] = [A^{-1}]^T \int_V [Q(x,y)]^T [D].[Q(x,y)].dV.[A]^{-1} = [A^{-1}]^T [K_o].[A]^{-1} \qquad [31]$$

The evaluation of the expression $[K_0]$ is determined by analytic integration of the various components of the resulting matrix product $[Q(x,y)]^T[D].[Q(x,y)]$. whose expressions take the form "$H_{\alpha\beta} = C.x^{\alpha}.y^{\beta}$". The matrix $[K_o]$ on the element "HIMEUR" is appended. So the matrix $[K_o]$ is evaluated by analytical integration of values $\int_x \int_y H_{\alpha\beta} = \int_x \int_y C.x^{\alpha}.y^{\beta}$. Finally, the elementary stiffness matrix, to be considered at the assembly and construction of the global stiffness matrix of the structure, is obtained after condensation of the matrix $[K^e]$. The static condensation is related at the freedom degrees to the fictitious fourth node.

4. Validation of the element "HIMEUR"

4.1. *Patch-tests*

4.1.1. *Rigid modes Patch-test*

This test is performed on one single element. The aim is to check the representation of rigid body motions of our element. To do this we define three vectors $\{Ut_i\}$, $\{Uxz_i\}$ $\{Uyz_i\}$ corresponding to the rigid modes. Then, we checked for each mode, provided that: $[K]\{Un\}=\{0\}$. The vectors considered are:

– Translation rigid mode : $<Ut_i>$ = < 1 0 0 1 0 0 1 0 0>

– Rotation rigid mode in "*xz*" : $<Uxz_i>$ = <-x_1 1 0 -x_2 1 0 -x_3 1 0>

– Rotation rigid mode in "*yz*" : $<Uyz_i>$ = <-y_1 0 1 -y_2 0 1 -y_3 0 1>

To see also the influence of geometric distortion, we tested several geometric shapes (isosceles triangle, rectangular triangle and any form of lowered). The results show that for our part there is a good representation of rigid body motions, since the condition [K]{U*n*}={0} is satisfied whatever the geometry of the element.

4.1.2. *Mechanical Patch-test*

We consider, on this test, an assembly of four triangular elements on a rectangular domain of sides 2a and 2b = 40 units = 20 units. We impose on the contour of this domain a Stresses reflecting the constant moments (or stress) state defined as shown in Figure 3.

Other data of the problem are: *E=1000; v=0.3; h=0.01 – 0.04 – 1.0 – 4.0; $W_1=W_2=W_3=0$*

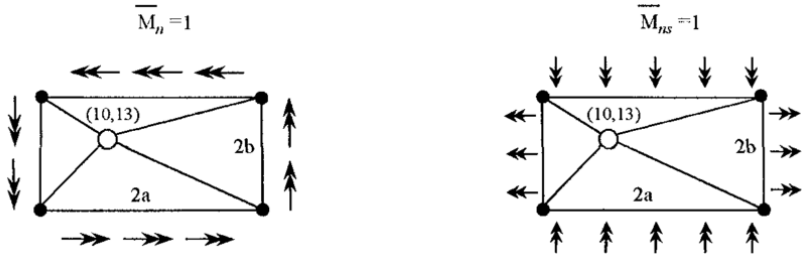

(a) Stresses on the contour reflecting the constant stress state

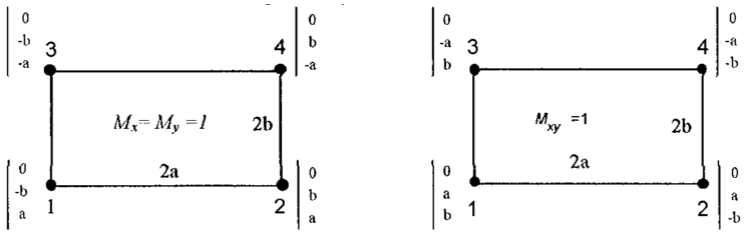

(b) Equivalent nodal forces

Figure 3. "*Mechanical" Patch test of element Kirchhoff type*

After calculating the stiffness matrix, assembly, taking into accounts the boundary conditions and the resolution we get to nodes 4 and 5, the results given in Table 1. From these results we conclude that our element passes with success this patch test.

Table 1. *Results of "mechanical" Patch test of element Kirchhoff type*

Thickness		h=0.01	h=0.04	h=1.0	h=4.0
$\overline{M}_x = \overline{M}_y = 1$	$M_{x(node\ 05)}$	0.98	0.98	0.98	0.98
	$M_{y(node\ 05)}$	-1	-1	-1	-1
$\overline{M}_{xy} = 1$	$M_{xy(node\ 05)}$	-0,97	-0,97	-0,97	-0,97

4.2. *Twisting of a square plate*

This problem is used to evaluate the ability of the HIMEUR element to represent a constant twisting. The same problem has been considered in references (Yuan *et al*., 1988), (Clough *et al*., 1965) and (Batoz *et al*., 1980). The plate in Figure 4 is simply supported (W=0) at the corners B, C and D. A transverse force of P=5 lb is applied at corner A. Young's modulus is 10.000 psi, Poisson's ratio is 0.3 and the thickness and the length of the plate are 1.0 and 8.0 in., respectively. The exact solution using thin plate theory is W_A =0.24960 in. and W_F =0.06240 in. at the centre of the plate, M_{xy} =2.5 lb in/in. and M_x = M_y =0 everywhere in the plate.

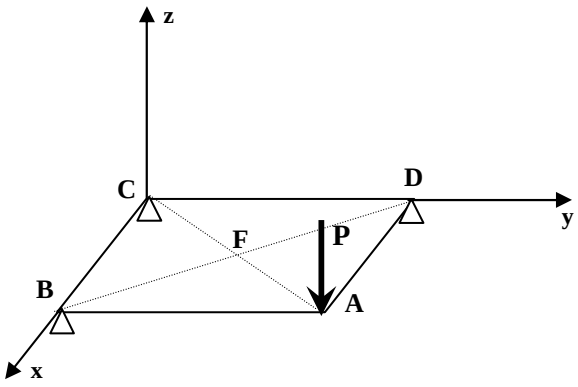

Figure 4. *Twisting of a square plate*

Results for the deflections at point A and F, and for the moments M_x, M_y and M_{xy} everywhere in the plate are presented in Table 2 with those of other elements given in references (Yuan *et al*., 1988), (Clough *et al*., 1965) and (Batoz *et al*., 1980). The results for the HIMEUR element are excellent, and the four meshes give the exact solution for the stresses and deflections.

Table 2. *Twisting of a square plate – Deflections at point A and F*

Element type	Deflection at		Moments in the plate	
	Point A	Point F	Point A	Point F
HIMEUR (4 meshes)	0.24960	0.06240	0	-
ACM (Clough *et al*., 1965) (8x8)	0.24972	0.06244	-	-
HCT (Clough *et al*., 1965) (8x8)	0.25002	0.06254	-	-
DKT (Batoz *et al*., 1980)	0.24960	0.06240	0	2.5
HSM (Batoz *et al*., 1980)	0.24960	0.06240	0	2.5
Exact solution (Thin theory)	0.24960	0.06240	0	2.5

4.3. *Cantilever beam subjected to point load at its free end*

This test checks the behaviour of our simple bending element based on the slenderness ratio (*L/h*). Indeed, in this case the bending test before the shear is dominant for ratios *L/h* rates. At the free end, the beam is subjected in the direction "*Oz*" to *A* point load of intensity *P = 0.1*. It simulates a perfect fitting to the other end (see Figure 5).

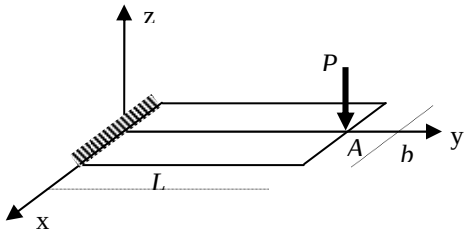

Figure 5. *Cantilever beam subjected to point load*

Geometric data and mechanical loading are given in Table 3.

Table 3. *Geometric and mechanical loading for the cantilever beam in simple bending*

Length	L=10.0
Width	b=1.0
Thickness	h= (L/100 ≈ L)
Young's modulus	$E=1.2x10^6$
Poisson	$\nu = 0.0$
Loading	P=0.1

To see the influence of transverse shear on the behaviour of our element, we simulate in this test case, the displacement "w" from point "A" under the direction of "Oz" for several values of the ratio L/h.

We then compare the results, first to the theoretical solution given by (32) of the beam theory and on the other hand, the behaviour of other triangular elements treated Guenfoud DSTM, ANST6, DKTM (Guenfoud, 1993).

The theoretical solution of the displacement "w" from point "A" in direction "Oz" is given as follows:

$$w_t = \frac{4PL^3}{Ebh^3}\left[1+\frac{1}{2k}\left(\frac{h}{l}\right)^2\right] \qquad \text{with k=5/6} \qquad [32]$$

The simulation results point "*A*" in the direction "*Oz*" is given in Figure 5 and Table 4.

Table 4. *Displacement from point A along the axis "Oz" of the cantilever beam in simple bending*

L/h	DSTM	ANST6	DKTM	HIMEUR	Theoretical solution
2	2.9x10-6	3.0x10-6	2.5x10-6	2.7x10-6	3.1x10-6
3	9.0x10-6	9.6x10-6	8.4x10-6	9.0x10-6	9.6x10-6
4	2.0x10-5	2.2x10-5	2.0x10-5	2.1x10-5	2.2x10-5
5	4.0x10-5	4.2x10-5	3.9x10-5	4.1x10-5	4.3x10-5
10	-	-	-	3.3x10-4	3.3x10-4
100	0.31329	-	0.31327	0.33303	0.3333

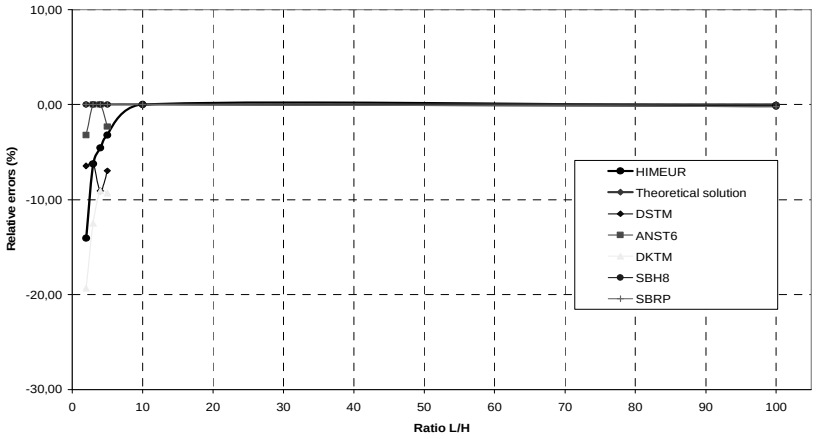

Figure 6. *Relative errors of displacement "W" on point A in pure bending*

Figure 6 shows, in graphic form, the standard displacement of point "A" in simple bending function of the ratio L/h and comparing the behaviour of the element HIMEUR from the theoretical benchmark solution. We note that our element is very efficient for large slenderness (L/h> 10). It should be noted that its convergence to the solution is obtained with a mesh consisting of ten (10) elements. Table 4 also summarizes the results given by other existing triangular elements. We note here also that our element is robust to the elements DSTM (Guenfoud, 1993) and DKTM (Guenfoud, 1993) especially for L/h> 3, since its behaviour is closer to the theoretical benchmark solution.

4.4. *Isotropic square plate*

This example (see Figure 7) was taken by many authors in the literature including (Batoz *et al*., 1990). This is an isotropic square plate of side *a* and thickness *h*. In this work we simulate several scenarios based on the boundary conditions of the plate and the type of loading. It is in this test case to study the behaviour of the element HIMEUR considering different mesh sizes and several ratios "*a/h*".

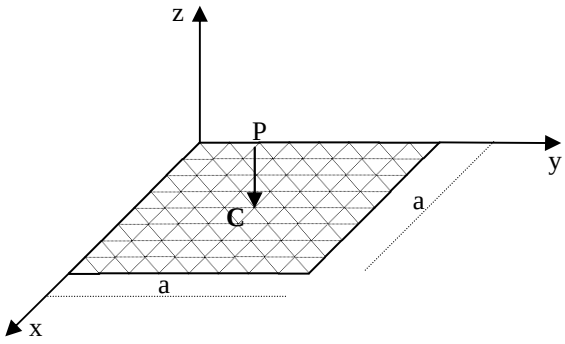

Figure 7. *Isotropic square plate subjected to point load applied at its centre*

The results concerning the displacement "w" the central point (C) of the plate is compared to analytical solutions for thin plate's data for each case. As we proceed with comparisons with triangular elements in the existing literature, including elements SRI (Sabourin *et al*., 2000), C^O (Belytschko, 1984), TRUMP (Argyris *et al*., 1977), DKT (Batoz *et al*., 1990).

4.4.1. *Isotropic square plate requested by a point load applied at its centre*

4.4.1.1. Isotropic square plate simply supported on all four sides

Geometric and mechanical data are given in Table 5.

Table 5. *Geometric and mechanical loading for the isotropic square plate, simply supported on all four sides, with concentrated load at point C*

Length	a = 2.0m
Thickness	h= 0.03m
Young's modulus	E=210x10^{9}N/m²
Poisson	ν = 0.3
Loading	P= 800 N

The theoretical solution of the displacement "*w*" from point "*C*" along the direction of "*Oz*" is given by (Batoz *et al*., 1990) as follows:

$$w_t = 0.0116\frac{Pa^2}{D} \qquad \text{with} \qquad D = \frac{Eh^3}{12\left(1-\nu^2\right)} \qquad [33]$$

The results of the displacement of point "*C*" following direction "*Oz*" with different meshes is shown in Figures 8; 9 and Table 6.

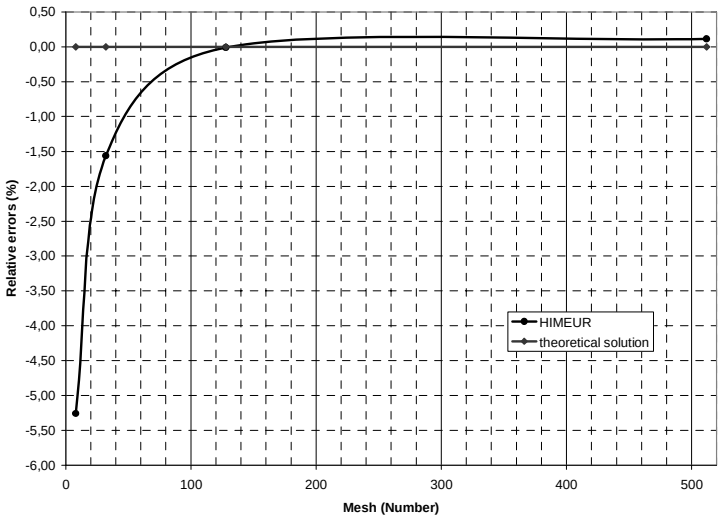

Figure 8. *Relative errors of displacement "W" on point C - isotropic square plate, simply supported on all four sides, with concentrated load at point C*

Table 6. *Normalized Displacement "Wc/Wt" Point C - isotropic square plate, simply supported on all four sides, with concentrated load at point C*

Mesh	4 x 4			6 x 6			8 x 8		
a/h	**100**	**1000**	**10000**	**100**	**1000**	**10000**	**100**	**1000**	**10000**
SRI	0.070	0.9E-3	0.9E-5	0.134	0.0018	1.9E-5	0.207	0.0031	3.1E-5
C^O	0.898	0.382	0.008	0.960	0.781	0.083	0.978	0.916	0.309
TRUMP	1.017	1.016	1.016	1.009	1.007	1.007	1.006	1.004	1.004
DKT	1.003	1.003	1.003	1.002	1.002	1.002	1.001	1.001	1.001
HIMEUR	0.984	0.984	0.984	0.997	0.997	0.997	1.000	1.000	1.000

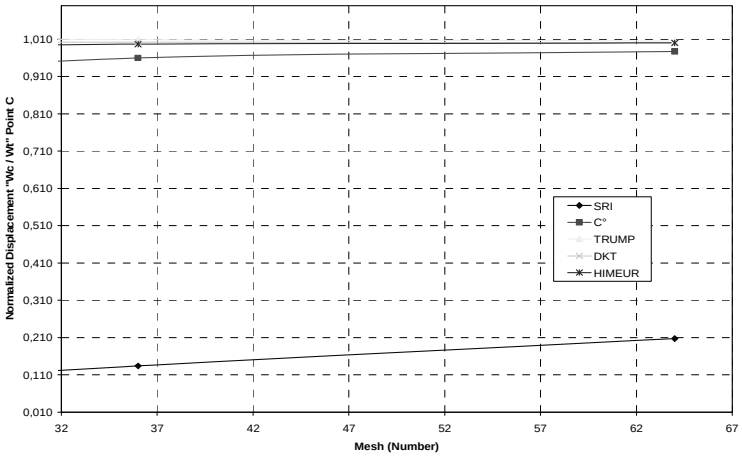

Figure 9. *Normalized Displacement "Wc/Wt" Point C (a/h = 100) - isotropic square plate, simply supported on all four sides, with concentrated load at point C*

Figure 8 shows, in graphic form, displacement from point "*C*" with different meshes. We note the good performance of our element, since it converges rapidly towards the analytical solution of reference.

Table 6 and Figure 9 also includes the values of the normalized displacement "*Wc/Wt*" of point *C* of some elements of triangular thin plate, for different meshes and several reports "*a/h*" and highlights the quality of results obtained by the element HIMEUR to these elements. Again this element is more robust than the elements SRI (Sabourin *et al.*, 2000), C^O (Belytschko, 1984), TRUMP (Argyris *et al.*, 1977), whatever the mesh or the ratio "*a/h*" and is very competitive with the DKT element (Batoz *et al.*, 1990).

4.4.1.2. Isotropic square plate clamped at its four sides

We resume the test case for this example in Figure 5 with the same geometrical and mechanical data of the material, but simulating a perfect fitting of the plate on all four sides. The theoretical solution of the displacement "*w*" from point "*C*" along the direction of "*Oz*" is given by (Batoz *et al*., 1990) as follows:

$$w_t = 0.0056\frac{Pa^2}{D} \qquad \text{with} \qquad D = \frac{Eh^3}{12\left(1-\nu^2\right)} \qquad [34]$$

The results of the displacement of point "*C*" following direction "*Oz*" with different meshes are shown in Figure 9.

The Figure 10 shows, graphically, the displacement from point "*C*" with different meshes. Just as the previous test cases, our present element, there is also a good performance, since it converges rapidly towards the analytical solution of reference.

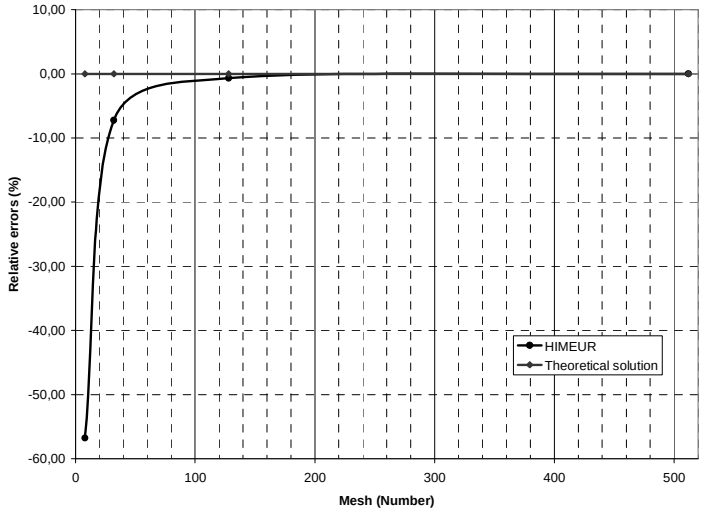

Figure 10. *Relative errors of displacement "W" on point C - isotropic square plate clamped at its four sides, with concentrated load at point C*

4.4.2. *Isotropic square plate requested by a uniformly distributed load*

We resume for this test case the sample plate of Figure 7 that we are seeking a uniformly distributed load of intensity *q=60 T/sqm*.

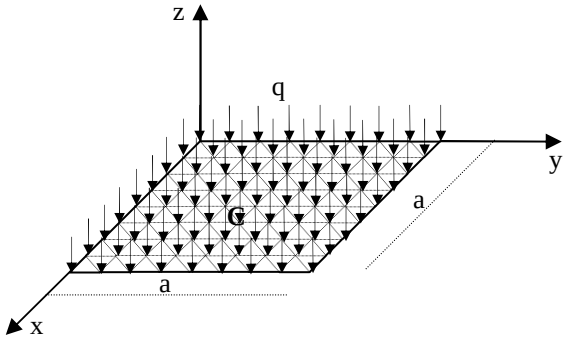

Figure 11. *Square isotropic plate subjected to a uniformly distributed load*

The theoretical solution of the displacement "*w*" from point "*C*" along the direction of "*Oz*" is given for the case of a plate simply supported by the formula [35] and for the case of the plate embedded in the formula (36):

$$w_t = 0.004062\,\frac{qa^4}{D} \qquad \text{with} \qquad D = \frac{Eh^3}{12\left(1-\nu^2\right)} \qquad [35]$$

$$w_t = 0.00126\,\frac{qa^4}{D} \qquad \text{with} \qquad D = \frac{Eh^3}{12\left(1-\nu^2\right)} \qquad [36]$$

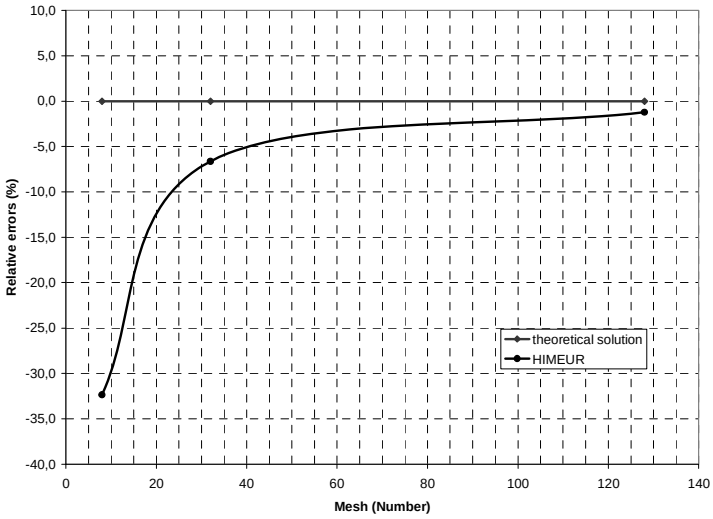

Figure 12. *Relative errors of displacement "W" on point C - isotropic square plate simply supported on all four sides with a uniformly distributed load*

The simulation results of displacement of point "*C*" following direction "*Oz*" with different meshes are shown in Figures 12 and 13. Figure 12 summarizes the results for the case of a plate simply supported and Figure 13 summarizes the results for the plate clamped along its four sides. We note that for both test cases, our element behaves well, since it is characterized by rapid convergence to the analytical solution.

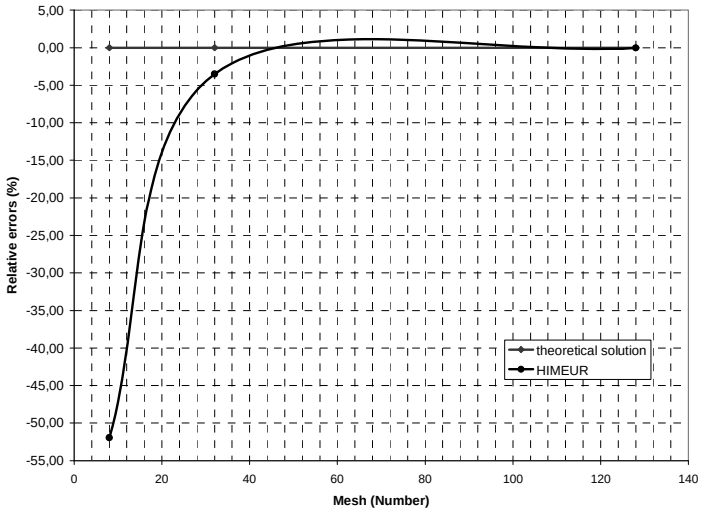

Figure 13. *Relative errors of displacement "W" on point C - Isotropic square plate clamped at its four sides, with a uniformly distributed load*

4.5. *Skew isotropic plate*

It is for this test, a plate of isotropic skew (corner 60 °) (Figure 14) subjected to a uniform load p with two simple supports (W = 0) and two free edges. Geometric and mechanical data are given in Table 7.

Table 7. *Data geometric, mechanical bias for the plate (60 °) isotropic*

Side length	L = 100.0
Thickness	h= 0.1
Young's modulus	E=1000
Poisson	ν = 0.31

This problem treated by (Batoz *et al.*, 1990) for the analysis of quadrilateral elements and DSQ Q4γ is used to evaluate the convergence of our element. To do this we considered grids of 2x2, 4x2, 8x2, 16x2 elements per side.

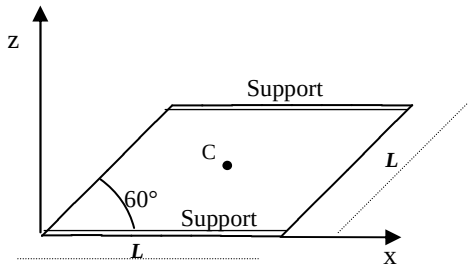

Figure 14. *Isotropic skew plate (60 °) with free edges*

The reference solution, obtained by a finite difference scheme (Razake, 1973), is given by formula 37.

$$w_{ref} = 0.07945 \frac{Pl^2}{D} \qquad \text{with} \qquad D = \frac{Eh^3}{12\left(1-\nu^2\right)} \qquad [37]$$

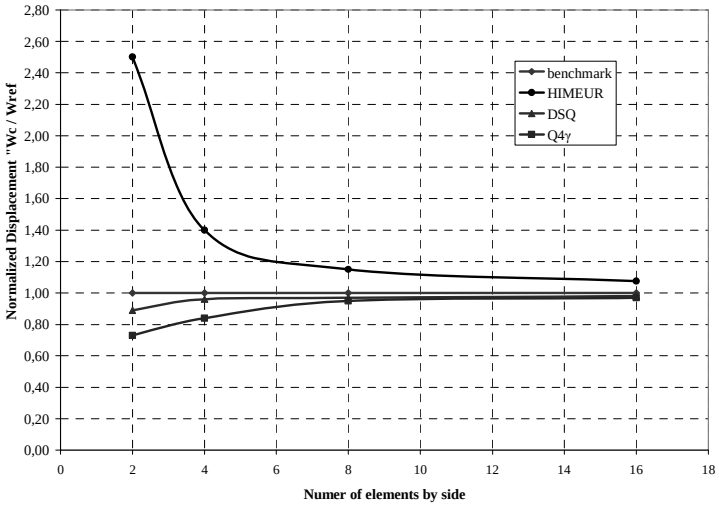

Figure 15. *Normalized Displacement "Wc/Wref." the central point - isotropic plate with free edges skew*

The results of displacements obtained by the element HIMEUR are illustrated by the Figure 15. We've also worn for purposes of comparison, the results given by the elements and quadrilateral DSQ Q4γ (Batoz *et al.*, 1990). We observe a monotonic convergence for all three items with a convergence at the top of the element "HIMEUR".

4.6. *ROBINSON Tests*

There are two tests proposed by Robinson (Robinson, 1978) to study the behaviour of a triangular element loaded in bending and torsion constrained.

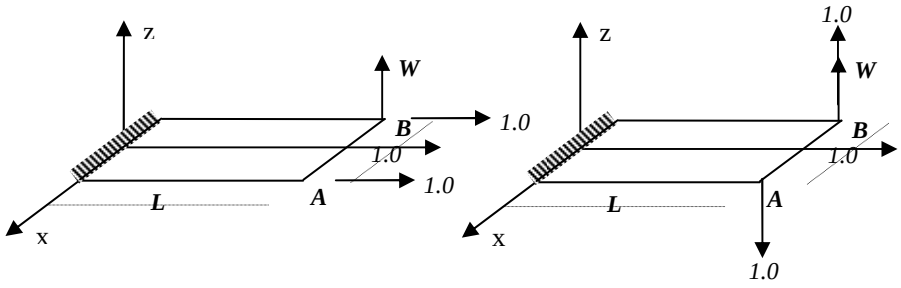

a - 16.1 - bending constrained **b - 16.2 - twisting constrained**

Figure 16. *Cantilever beam subjected to ROBINSON tests*

The geometrical and mechanical characteristics of the material are given in Table 8. We study the influence of the ratio L/h (the length varies from 1 *x* h to 10000 *x* h) on the move "*W*" from point "*A*" for both types of solicitations.

Table 8. *Geometric, mechanical material for the cantilever beam submitted to test ROBINSON*

Side length	L = Variable
Width	b=1.0
Thickness	h= 0.05
Young's modulus	$E=1.0x10^7$
Poisson	$\nu = 0.25$

Test "A" for the behaviour of the cantilever beam under the action of two pairs $M_y = 1.0$ applied to the nodes of its free end. This is the bending constrained. Test "B" for the action of two concentrated loads $P_z = -1.0$ and $P_z = 1.0$ respectively

applied to the same nodes. This is the twisting constrained. The reference solution (BENCHMARK) on triangular elements is extracted from (Guenfoud, 1990).

Table 9. *Test "A" – Bending constrained - displacement "W" from point "A"*

L	ANST3	ANST6	HCT	DKT	HIMEUR	BENCHMARK
0.05	0.00000174	0.0000064	-	-	0.000008022	-
0.5	0.00087300	0.0011800	-	-	0.00092053	-
1	0.00356000	0.0038100	0.0010520	0.002105	0.00235240	0.0028
2	0.00935000	0.0100000	0.0015790	0.006580	0.00614230	0.0056
3	0.01480000	0.0162000	0.0010520	0.009870	0.00938960	0.0084
4	0.02020000	0.0222000	0	0.013160	0.01215900	0.0112
5	0.02550000	0.0280000	-0.0052600	0.016450	0.01477200	0.0140
6	0.03070000	0.0339000	-0.0018420	0.019740	0.01735700	0.0168
7	0.03600000	0.0397000	-	0.023030	0.01995100	0.0196
8	0.04120000	0.0455000	-0.0028940	0.026320	0.02256200	0.0224
9	0.04600000	0.0513000	-	0.029620	0.02518800	0.0252
10	0.05170000	0.0571000	-0.0044730	0.032900	0.02782800	0.0280
11	-	-	-	0.036190	0.03047800	0.0308
12	-	-	-0.0057890	0.039480	0.03313700	0.0336
25	0.12970000	0.1433000	-	-	0.06805900	-
50	0.25970000	0.2869000	-	-	0.13567000	-
500	2.59850000	2.6540000	-	-	1.35530000	-

Table 10. *Test "B" - Twisting constrained - displacement "W" from point "A"*

L	ANST3	ANST6	HCT	DKT	HIMEUR	BENCHMARK
0.05	0.00000116	0.00000383	-	-	0.00000100	-
0.5	0.00043800	0.00088300	-	-	0.00045531	-
1	0.00178000	0.00252000	0.0010660	0.001866	0.00186770	0.002666
2	0.00467000	0.00555000	0.0024000	0.004400	0.00550220	0.005333
3	0.00743000	0.00847000	0.0030660	0.006800	0.00840630	0.007999
4	0.01010000	0.01130000	0.0034660	0.009200	0.01095800	0.010666
5	0.01270000	0.01420000	0.0037330	0.011733	0.01344500	0.013333
6	0.01540000	0.01710000	0.0042666	0.014000	0.01593200	0.015999
7	0.01800000	0.02000000	-	0.016400	0.01842900	0.018666
8	0.02060000	0.02290000	0.0050660	0.018933	0.05093700	0.021333
9	0.02320000	0.02570000	-	0.021333	0.02345500	0.023999
10	0.02580000	0.02860000	0.0061330	0.023600	0.02598100	0.026666
11	-	-	-	0.025866	0.02851200	0.029333
12	-	-	0.0070660	0.028266	0.03104700	0.031999
25	0.06489000	0.07170000	-	-	0.06419500	-
50	0.12986000	0.14350000	-	-	0.12817000	-
500	1.29930000	1.43270000	-	-	1.28090000	-

Tables 9 and 10 and Figures 17 and 18 show the displacement "*W*" from point "*A*" according to the ratio L/h and comparing the behaviour of the element HIMEUR compared to the reference solution (BENCHMARK) and the results given by other existing triangular elements ANST3 (Guenfoud, 1990) ANST6 (Guenfoud, 1990), HCT, DKT (Batoz *et al*., 1990). The detailed study of the results highlights the good performance of the element HIMEUR. Indeed the results achieved are very close to

the reference solution for both constrained for bending torsion constrained and this regardless of the length "L". It should be noted that this result is obtained with a moderate mesh consisting only of four triangular elements. Moreover, the element HIMEUR appears stronger than all the elements taken as a basis for comparison, although the element DKT for the situation constrained bending and to a lesser extent the ANST3 element for the situation of twist embarrassed it are competitive. Figures 17 and 18 illustrate graphically these findings.

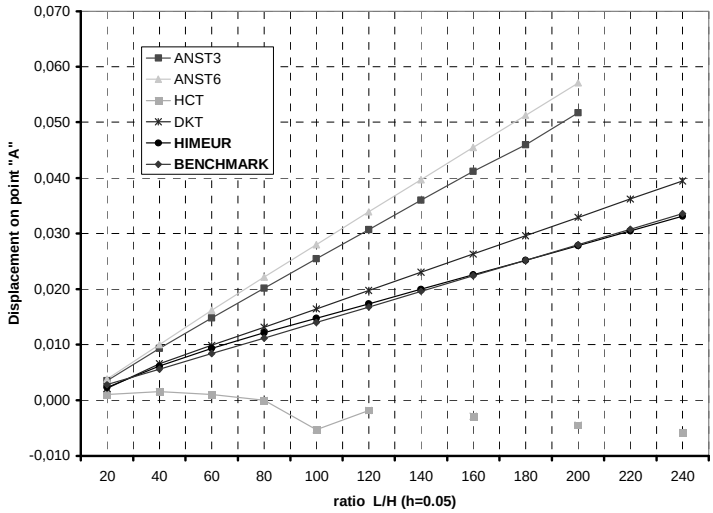

Figure 17. *Test "A" - Bending constrained - displacement "W" from point "A"*

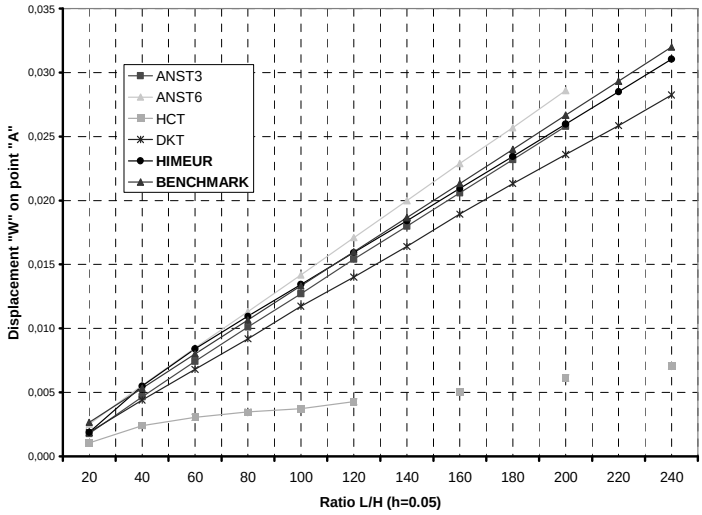

Figure 18. *Test "B" - Twisting constrained - displacement "W" from point "A"*

4.7. *Influence of the distorted meshes*

This event test checks the behaviour of the element when we are in the presence of a geometrically distorted mesh. Being a thin plate element, we considered a test case where it dominates the bending to shear. Indeed, it is a beam subjected to the right end, a shear force P = 4 N in the vertical direction Oz. This load is distributed appropriately to nodes of the right end. It simulates a perfect fitting to the left end of the beam (see Figure 19).

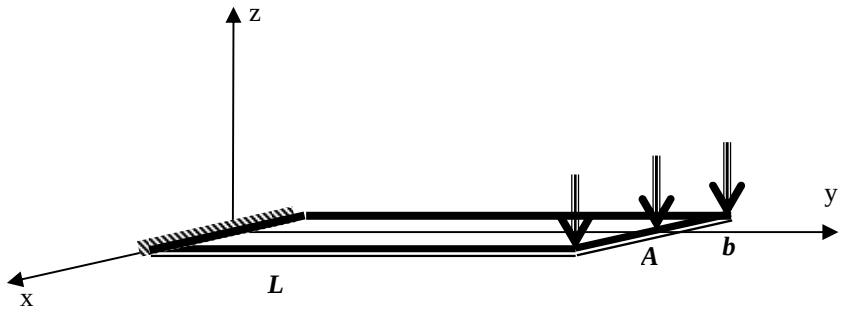

Figure 19. *Beam subjected to point load*

Geometric data and mechanical loading are given in Table 11.

Table 11. *Geometric and mechanical loading for the cantilever beam in simple bending*

Length	L = 50 m
Width	b = 4 m
Thickness	h = 1 m
Young's modulus	E = 6,825x10^7
Poisson	ν = 0.3
Loading	P = 4 N

The displacement "*W*" from point A in the end is found analytically and results from the strength of materials as it is expected that the removals are low compared to the length of the beam (of small perturbations and linear elastic behaviour). This is given as fallows:

$$w_t = \frac{P.L^3}{3E.I} \qquad \text{with} \qquad I = \frac{b.h^3}{12} \qquad [38]$$

The configuration of the mesh considered is shown in the diagram below:

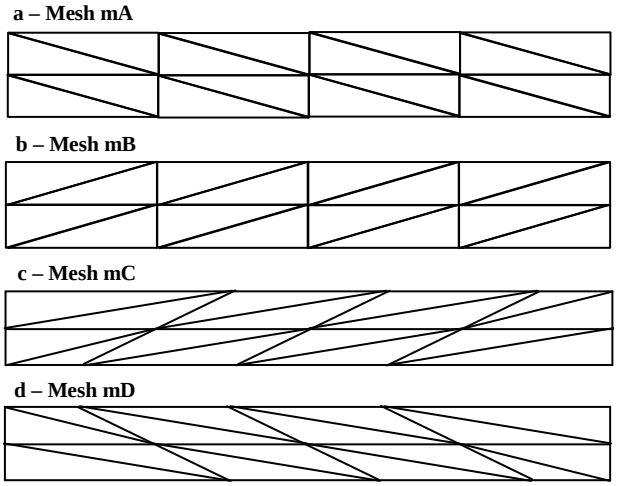

Figure 20. *Cantilever beam subjected to point load*

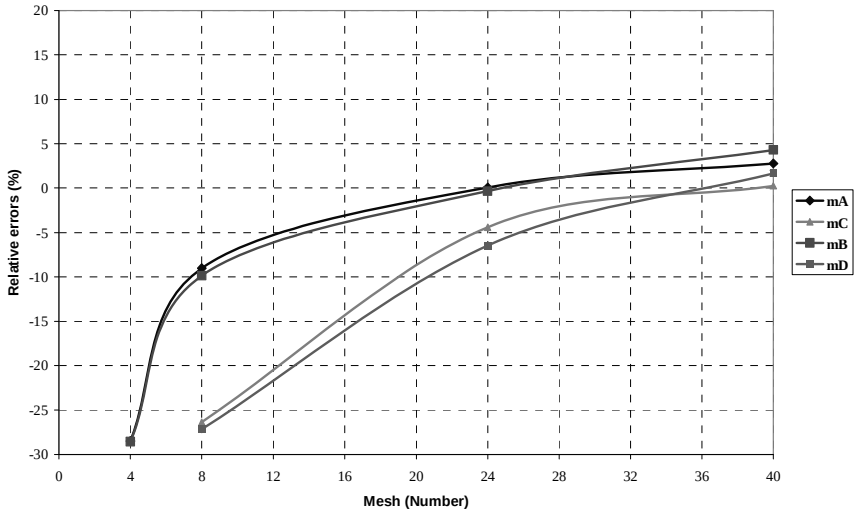

Figure 21. *Influence of the distorted meshes - Relative errors of displacement "W" on point A*

The results of the displacement of point "*A*" following direction "*Oz*" with different meshes is shown in Figure 21. We note that our element converges quickly for regular meshes "mA" and "mB". Thus, there is also no significant effect on the orientation of the grid: the ratio W_B / W_A is between 0.990 and 1.014 depending on the density of the mesh.

Also, the results show that the Himeur element is insensitive to geometric distortion ("mC" and "mD"), especially for an optimum density of the mesh. For a mesh of N = 40, the influence is 2.45%.

5. Conclusion

In this work, we have presented a triangular inflected finite element in the perspective of linear static analysis and dynamic analysis for the geometric non linear of curved structures (arch and shell). The adopted approach and the development of concepts and techniques used have allowed us to come to a competitive, robust and efficient finite element for the treatment of thin plates.

It remains that its maturation is carried on to make of it a reliable and efficient tool so as to address the calculation of all situations of shells, from thin to thick, deep or shallow ones. It is an element which shows undoubted advantages which plead to its use. The presence of the fictitious node and the adoption of the deformation approach have given the opportunity of enriching the displacement fields, and consequently, a greater accuracy in the approximation of the solution by avoiding the complexity of the classical theories. The reduction of elementary stiffness matrices by the means of the "static condensation" technique is an action relating to the freedom degrees related to the fictitious node, and which allows the avoidance of enormous systems of equations to be solved. Therefore, non negligible savings of time are recorded. The use of analytical integration in the evaluation of the stiffness matrix, gave our element a behaved performance. This result was remarkable in the convergence tests carried out where we have noticed a rapid trend towards the solution contrary to the isoperimetric elements (using numerical integration).

6. References

Argyris J. H., Dune P. C., Malejannakis G.A., Schelkle E., "A simple triangular facet shell element with applications to linear and non linear equilibrium and elastic stability problems", *Computer Methods in Applied Mechanics and Engineering*, vol. 10, n° 3, March 1977, p. 371-403.

Barik M., Mukhopadhyay M., "A new stiffened plate element for the analysis of arbitrary plates", *Thin-Walled Structures*, vol. 40, n° 7-8, 2002, p. 625-639.

Batoz J. L., Dhatt G., *Modélisation des structures par éléments finis*, vol. 1, *Solides Elastiques*, vol. 2, *Poutres et plaques*, Hermès, Paris, 1990.

Batoz J. L., Bath KJ, Ho L.W., "A study of three node triangular plate bending elements", *Int. J. Num. Meth. Eng*., 15, 1980, p. 1771-812.

Belarbi M. T., Développement de nouveaux éléments à modèle en déformation : Application linéaire et non linéaire, Thèse de Doctorat, Université de Constantine (Algérie), 2000.

Belarbi M. T., Charif A. « Développement d'un nouvel élément hexaédrique simple basé sur le modèle en déformation pour l'étude des plaques minces et épaisses », *Revue européenne des éléments finis*, 1999, p. 135-157.

Belytschko T. Ong J.S.J. Liu, WK., Kennedy J.M., "Hourglass control in linear and nonlinear problems", *Computer methods in applied mechanics and engineering*, vol. 43, 1984, p. 251-276.

Belounar L., Guenfoud M., "A new rectangular finite element based on the strain approach for plate bending", *Thin-Walled struct*., vol. 43, 2005, p. 47-63.

Chinosi C., "PSRI elements for the Reissner–Mindlin free plate", *Computers & Structures*, vol. 83, n° 31-32, December 2005, p. 559-2572.

Clough R.W., Tocher JL., "Finite element stiffness matrixes for analysis of plate bending, Proceeding of first conference Matrix methods in structural mechanics", *Wright-Pattersonm Qir force basem Ohiom*, 1965, p. 515-812.

Do-Nyun Kim, Klaus-Jürgen Bathe, "A triangular six-node shell element", *Computers & tructures*, vol. 87, n° 23-24, December 2009, p. 1451-1460.

François Frey, *Traité de génie civil de l'école polytechnique fédérale de Lausane – Volume 3 – Analyse des structures et milieux continus – mécanique des solides*, Presses polytechniques et universitaires romandes Ch. 1015, 1998.

Guenfoud M., Présentation de l'élément DSTM pour le calcul linéaire des coques d'épaisseur quelconque, Ann. l'ITBTP, 1993, 515, p. 25-52.

Guenfoud M., Deux éléments triangulaires nouveaux pour l'analyse linéaire et non linéaire géométrique des coques, Thèse de doctorat, Institut national des sciences appliquées de Lyon (France), Novembre 1990.

Hamadi D. J. and Belarbi M. T., "Integration solution routine to evaluate the element stiffness matrix for distorted shape", *Asian journal of civil engineering (Building housing)*, vol. 7, n° 5, 2006, p. 525-549.

Himeur M., Développement d'éléments membranaires nouveaux d'élasticité plane basés sur la formulation en déformation, Thèse de magistère, Université de Guelma (Algérie), Département de Génie Civil, Novembre 2008.

Himeur M., Guenfoud M., « Elément fini triangulaire nouveau à nœud central perturbé en formulation déformation avec drilling rotation », *CIFMA'03*, 21-23 Avril 2008, Alep, Syrie.

Ibrahimbegovic A., et Frey F. et Rebora B., Une approche unifiée de la modélisation des structures complexes : les éléments finis avec degré de liberté de rotation, LSC, Rapport Interne 93/10, Ecole polytechnique fédérale de Lausanne (Suisse), Juin 1993.

Maalem T., Contribution au modèle en déformation dans l'analyse des structures, Thèse de Doctorat, Université de Batna (Algérie), 2007.

Messaoudi H., Approche unifiée pour la modélisation d'une buse enterrée, Mémoire de Magister, Université de Batna (Algérie), 2004.

Providas E. and Kattis M. A., "An assessment of two fundamental flat triangular shell elements with drilling rotation", *Computers and structures*, vol. 77, 2000, p. 129-139.

Razake A., “Program of triangular bending elements with derivative smoothing”, *IJNME*, vol. 6, 1973, p. 333-343.

Robinson J., “Element evaluation. A set of assessment points and standards tests Proc.”, *Element method in the commercial environment*, vol. 1, Oct. 1978, p. 217-248.

Sabir A.B., A Sfendji, “Triangular and Rectangular Plane Elasticity Finite Elements”, *Thin-Walled struct.*, vol. 21, 1995, p. 225-232.

Sabir A.B., “A rectangular and triangular plane elasticity element with drilling degrees freedom”, *chapter 9 in proceeding of the 2nd International conference on variational methods in engineering, Southampton University, Springer verlag*, Berlin, 1985, p. 17-25.

Sabir A.B., “A new class of finite elements for plane elasticity problems”, *CAFEM 7th, Int. conf. Struct. Mech. In reactor Tecnology*, Chicago, 1983.

Sabourin F.m Salle F., *Calcul des structures par éléments finis, Barres – Poutres Elasticité plane Axisymétrique Plaques – coques non linéarité*, Chapitre IV, INSA Lyon, 2000.

SARF J. L., La condensation statique dans felina (nouvelle édition), Rapport Interne LSC 91/22, 1991.

Teodorecu P., Grands éléments finis”GEF” pour l’élasticité plane, Thèse n° 462 de doctorat présentée au département de génie civil, Ecole polytechnique fédérale de Lausane Suisse, 1982.

Yuan F.,Miller RE., “A rectangular finite element for moderately thick flat plate”, *Computer Struct.* 1988, 30, p. 1375-87.

7. Appendix

A.1. Matrix of nodal coordinates

$$[A]=\begin{Bmatrix} w(x_1,y_1)\\ \beta_x(x_1,y_1)\\ \beta_y(x_1,y_1)\\ w(x_2,y_2)\\ \beta_x(x_2,y_2)\\ \beta_y(x_2,y_2)\\ w(x_3,y_3)\\ \beta_x(x_3,y_3)\\ \beta_y(x_3,y_3)\\ w(x_4,y_4)\\ \beta_x(x_4,y_4)\\ \beta_y(x_4,y_4) \end{Bmatrix} = \begin{bmatrix} 1 & -x_1 & -y_1 & -\frac{x_1^2}{2} & -\frac{x_1^3}{6} & -\frac{x_1^2y_1}{2} & -\frac{x_1^3y_1}{6} & -\frac{y_1^2}{2} & -\frac{x_1y_1^2}{2} & -\frac{y_1^3}{6} & -\frac{x_1y_1^3}{6} & -\frac{x_1y_1}{2}\\ 0 & 1 & 0 & x_1 & \frac{x_1^2}{2} & x_1y_1 & \frac{x_1^2y_1}{2} & 0 & \frac{y_1^2}{2} & 0 & \frac{y_1^3}{6} & \frac{y_1}{2}\\ 0 & 0 & 1 & 0 & 0 & \frac{x_1^2}{2} & \frac{x_1^3}{6} & y_1 & x_1y_1 & \frac{y_1^2}{2} & \frac{x_1y_1^2}{2} & \frac{x_1}{2}\\ 1 & -x_2 & -y_2 & -\frac{x_2^2}{2} & -\frac{x_2^3}{6} & -\frac{x_2^2y_2}{2} & -\frac{x_2^3y_2}{6} & -\frac{y_2^2}{2} & -\frac{x_2y_2^2}{2} & -\frac{y_2^3}{6} & -\frac{x_2y_2^3}{6} & -\frac{x_2y_2}{2}\\ 0 & 1 & 0 & x_2 & \frac{x_2^2}{2} & x_2y_2 & \frac{x_2^2y_2}{2} & 0 & \frac{y_2^2}{2} & 0 & \frac{y_2^3}{6} & \frac{y_2}{2}\\ 0 & 0 & 1 & 0 & 0 & \frac{x_2^2}{2} & \frac{x_2^3}{6} & y_2 & x_2y_2 & \frac{y_2^2}{2} & \frac{x_2y_2^2}{2} & \frac{x_2}{2}\\ 1 & -x_3 & -y_3 & -\frac{x_3^2}{2} & -\frac{x_3^3}{6} & -\frac{x_1^2y_3}{2} & -\frac{x_3^3y_3}{6} & -\frac{y_3^2}{2} & -\frac{x_3y_3^2}{2} & -\frac{y_3^3}{6} & -\frac{x_3y_3^3}{6} & -\frac{x_3y_3}{2}\\ 0 & 1 & 0 & x_3 & \frac{x_3^2}{2} & x_3y_3 & \frac{x_3^2y_3}{2} & 0 & \frac{y_3^2}{2} & 0 & \frac{y_3^3}{6} & \frac{y_3}{2}\\ 0 & 0 & 1 & 0 & 0 & \frac{x_3^2}{2} & \frac{x_3^3}{6} & y_3 & x_3y_3 & \frac{y_3^2}{2} & \frac{x_3y_3^2}{2} & \frac{x_3}{2}\\ 1 & -x_4 & -y_4 & -\frac{x_4^2}{2} & -\frac{x_4^3}{6} & -\frac{x_4^2y_4}{2} & -\frac{x_4^3y_4}{6} & -\frac{y_4^2}{2} & -\frac{x_4y_4^2}{2} & -\frac{y_4^3}{6} & -\frac{x_4y_4^3}{6} & -\frac{x_4y_4}{2}\\ 0 & 1 & 0 & x_4 & \frac{x_4^2}{2} & x_4y_4 & \frac{x_4^2y_4}{2} & 0 & \frac{y_4^2}{2} & 0 & \frac{y_4^3}{6} & \frac{y_4}{2}\\ 0 & 0 & 1 & 0 & 0 & \frac{x_4^2}{2} & \frac{x_4^3}{6} & y_4 & x_4y_4 & \frac{y_4^2}{2} & \frac{x_4y_4^2}{2} & \frac{x_4}{2} \end{bmatrix}$$

*A.2. Matrix **[Ko]***

- General form

$$\mathbf{[\,Ko\,]} = \frac{Eh^3}{12\left(1-\nu^2\right)} \int\int \begin{pmatrix} 0 & 0 & 0 \\ 0 & 0 & 0 \\ 0 & 0 & 0 \\ 1 & 0 & 0 \\ x & 0 & 0 \\ y & 0 & 2x \\ xy & 0 & x^2 \\ 0 & 1 & 0 \\ 0 & x & 2y \\ 0 & y & 0 \\ 0 & xy & y^2 \\ 0 & 0 & 1 \end{pmatrix} \cdot \begin{bmatrix} 1 & \nu & 0 \\ \nu & 1 & 0 \\ 0 & 0 & \frac{(1-\nu)}{2} \end{bmatrix} \cdot \begin{pmatrix} 0 & 0 & 0 & 1 & x & y & xy & 0 & 0 & 0 & 0 & 0 \\ 0 & 0 & 0 & 0 & 0 & 0 & 0 & 1 & x & y & xy & 0 \\ 0 & 0 & 0 & 0 & 0 & 2x & x^2 & 0 & 2y & 0 & y^2 & 1 \end{pmatrix} dx\,dy$$

- Expanded form before analytic integration

$$[K_0] = \frac{E.h^3}{12.(1-\nu^2)} \times$$

$$\begin{bmatrix} 0 & 0 & 0 & 0 & 0 & 0 & 0 & 0 & 0 & 0 & 0 & 0 \\ & 0 & 0 & 0 & 0 & 0 & 0 & 0 & 0 & 0 & 0 & 0 \\ & & 0 & 0 & 0 & 0 & 0 & 0 & 0 & 0 & 0 & 0 \\ & & & 1 & x & y & x.y & \nu & \nu.x & \nu.y & \nu.x.y & 0 \\ & & & & x^2 & x.y & x^2.y & \nu.x & \nu.x^2 & \nu.x.y & \nu.x^2.y & 0 \\ & & & & & 4.x^2.d + y^2 & 2.x^3.d + x.y^2 & \nu.y & x.y.(\nu + 4.d) & \nu.y^2 & x.y^2.(\nu + 2.d) & 2.x.d \\ & & & & & & x^4.d + x^2.y^2 & \nu.x.y & x^2.y.(\nu + 2.d) & \nu.x.y^2 & x^2.y^2.(\nu + d) & x^2.d \\ & & & & & & & 1 & x & y & x.y & 0 \\ & & & & & Sym. & & & x^2 + 4.y^2.d & x.y & x^2.y + 2.y^3.d & 2.y.d \\ & & & & & & & & & y^2 & x.y^2 & 0 \\ & & & & & & & & & & x^2.y^2 + y^4.d & y^2.d \\ & & & & & & & & & & & d \end{bmatrix}$$

with : $d = \frac{(1-\nu)}{2}$

- *Expanded form after analytic integration*

$$[K_0] = \frac{E.h^3}{12.(1-\nu^2)} \times$$

$$\begin{bmatrix}
0 & 0 & 0 & 0 & 0 & 0 & 0 & 0 & 0 & 0 & 0 & 0 \\
 & 0 & 0 & 0 & 0 & 0 & 0 & 0 & 0 & 0 & 0 & 0 \\
 & & 0 & 0 & 0 & 0 & 0 & 0 & 0 & 0 & 0 & 0 \\
 & & & H_{00} & H_{10} & H_{01} & H_{11} & \nu.H_{00} & \nu.H_{10} & \nu.H_{01} & \nu.H_{11} & 0 \\
 & & & & H_{20} & H_{11} & H_{21} & \nu.H_{10} & \nu.H_{20} & \nu.H_{11} & \nu.H_{21} & 0 \\
 & & & & & 4.H_{20}.d + H_{02} & 2.H_{30}.d + H_{12} & \nu.H_{01} & H_{11}.(\nu + 4.d) & \nu.H_{02} & H_{12}.(\nu + 2.d) & 2.H_{10}.d \\
 & & & & & & H_{40}.d + H_{22} & \nu.H_{11} & H_{21}.(\nu + 2.d) & \nu.H_{12} & H_{22}.(\nu + d) & H_{20}.d \\
 & & & & & & & H_{00} & H_{10} & H_{01} & H_{11} & 0 \\
 & & & & & \textit{Sym.} & & & H_{20} + 4.H_{02}.d & H_{11} & H_{21} + 2.H_{03}.d & 2.H_{01}.d \\
 & & & & & & & & & H_{02} & H_{12} & 0 \\
 & & & & & & & & & & H_{22} + H_{04}.d & H_{02}.d \\
 & & & & & & & & & & & H_{00}d
\end{bmatrix}$$

with : $H_{\alpha\beta} = \iint X^{\alpha}.Y^{\beta} dx.dy$

Recepted: February 2011
Accepted: February 2012